LYMPHOID NEOPLASIA

Functional-genetic dissection of HDAC dependencies in mouse lymphoid and myeloid malignancies

Geoffrey M. Matthews,[1,2,*] Parinaz Mehdipour,[3,*] Leonie A. Cluse,[1,2] Katrina J. Falkenberg,[1,4,5] Eric Wang,[6] Mareike Roth,[4] Fabio Santoro,[3] Eva Vidacs,[1,2] Kym Stanley,[1,2] Colin M. House,[2] James R. Rusche,[7] Christopher R. Vakoc,[6] Johannes Zuber,[4,†] Saverio Minucci,[3,8,9,†] and Ricky W. Johnstone[1,2,†]

[1]Cancer Therapeutics Program, Peter MacCallum Cancer Centre, East Melbourne, Victoria, Australia; [2]Sir Peter MacCallum Department of Oncology, University of Melbourne, Parkville, Victoria, Australia; [3]Department of Experimental Oncology, European Institute of Oncology, Milan, Italy; [4]Research Institute of Molecular Pathology, Vienna Biocenter, Vienna, Austria; [5]Department of Pathology, University of Melbourne, Parkville, Victoria, Australia; [6]Cold Spring Harbor Laboratory, Cold Spring Harbor, NY; [7]Repligen Corporation, Waltham, MA; [8]Drug Development Program, European Institute of Oncology, Milan, Italy; and [9]Department of Biosciences, University of Milan, Milan, Italy

Key Points

- Genetic studies suggest HDAC3-selective suppression may prove useful for treatment of hematological tumors but will not induce apoptosis.
- Genetic and pharmacological cosuppression of HDAC1 with HDAC2 induces a potent pro-apoptotic response of tumor cells.

Histone deacetylase (HDAC) inhibitors (HDACis) have demonstrated activity in hematological and solid malignancies. Vorinostat, romidepsin, belinostat, and panobinostat are Food and Drug Administration–approved for hematological malignancies and inhibit class II and/or class I HDACs, including HDAC1, 2, 3, and 6. We combined genetic and pharmacological approaches to investigate whether suppression of individual or multiple *Hdac*s phenocopied broad-acting HDACis in 3 genetically distinct leukemias and lymphomas. Individual *Hdac*s were depleted in murine acute myeloid leukemias (MLL-AF9;Nras^{G12D}; PML-RARα acute promyelocytic leukemia [APL] cells) and Eμ-*Myc* lymphoma in vitro and in vivo. Strikingly, *Hdac*3-depleted cells were selected against in competitive assays for all 3 tumor types. Decreased proliferation following *Hdac*3 knockdown was not prevented by BCL-2 overexpression, caspase inhibition, or knockout of *Cdkn1a* in Eμ-*Myc* lymphoma, and depletion of *Hdac*3 in vivo significantly reduced tumor burden. Interestingly, APL cells depleted of *Hdac*3 demonstrated a more differentiated phenotype. Consistent with these genetic studies, the HDAC3 inhibitor RGFP966 reduced proliferation of Eμ-*Myc* lymphoma and induced differentiation in APL. Genetic codepletion of *Hdac*1 with *Hdac*2 was pro-apoptotic in Eμ-*Myc* lymphoma in vitro and in vivo and was phenocopied by the HDAC1/2-specific agent RGFP233. This study demonstrates the importance of HDAC3 for the proliferation of leukemia and lymphoma cells, suggesting that HDAC3-selective inhibitors could prove useful for the treatment of hematological malignancies. Moreover, our results demonstrate that codepletion of *Hdac1* with *Hdac2* mediates a robust pro-apoptotic response. Our integrated genetic and pharmacological approach provides important insights into the individual or combinations of HDACs that could be prioritized for targeting in a range of hematological malignancies. (*Blood.* 2015;126(21):2392-2403)

Introduction

Histone deacetylase (HDAC) inhibitors (HDACis) are gaining widespread use for treatment of hematological malignancies.[1,2] The majority of HDACis target class I and/or II HDACs[3] and it is unclear which isoforms are vital for tumor cell growth and/or survival. Moreover, it is yet to be established whether selective HDACis could improve antitumor efficacy and limit toxicity. HDACs modify the epigenome through regulated chromatin acetylation and are thought to control gene transcription.[4] HDACs regulate expression of *CDKN1A* in many tumor types and are important cofactors in acute myeloid leukemia-1 (AML1)-ETO-driven AML.[2,4-6] HDACs have therefore become promising targets for therapeutic intervention aiming to reverse aberrant epigenetic states associated with cancer.[7]

Several structurally diverse HDACis have been developed representing different chemical families and HDAC specificity.[1,3,8] Vorinostat (Zolinza; Merck), romidepsin (Istodax; Celgene), belinostat (Beleodaq; Spectrum Pharmaceuticals), and panobinostat (Farydak; Novartis) are Food and Drug Administration (FDA)–approved for cutaneous/peripheral T-cell lymphoma and refractory multiple myeloma.[9-12] There are 11 "classical" mammalian HDACs:[3,13,14] class I HDACs (HDAC1, 2, 3, 8) are located primarily within the nucleus; class IIa HDACs (HDAC4, 5, 7, 9) shuttle between the nucleus and the cytoplasm; and class IIb HDACs (HDAC6, 10) contain 2 catalytic domains and are exclusively found in the cytoplasm. HDAC6 has substrate specificity for α-tubulin and class IV (HDAC11) has characteristics of both class I and II HDACs. Vorinostat, panobinostat, and belinostat inhibit

Submitted March 7, 2015; accepted September 16, 2015. Prepublished online as *Blood* First Edition paper, October 7, 2015; DOI 10.1182/blood-2015-03-632984.

*G.M.M. and P.M. contributed equally to this study.

†J.Z., S.M., and R.W.J. contributed equally to this study.

The online version of this article contains a data supplement.

The publication costs of this article were defrayed in part by page charge payment. Therefore, and solely to indicate this fact, this article is hereby marked "advertisement" in accordance with 18 USC section 1734.

HDAC1, 2, 3, and 6, whereas romidepsin has high affinity for HDAC1, 2, and 3.[3]

HDACis mediate a range of biological responses including: apoptosis; inhibition of cell-cycle progression; cellular differentiation; suppression of angiogenesis; and enhancing antitumor immunity.[1] HDACs also regulate function, localization and/or stability of nonhistone proteins.[15-17] For example, the acetylation of heat shock protein-90 (HSP90), a molecular chaperone, is regulated by HDAC6.[18] As such, HSP90 client oncoproteins, including BCR-ABL and ERBB2, may be degraded via HDACi-mediated HSP90 deacetylation and have been proposed as a major effector of HDACi mechanism of action.[13] The combined effects of histone and nonhistone hyperacetylation are likely critical for the therapeutic activity of HDACis.[19]

HDAC-selective inhibitors are being developed in the hope of mediating potent antitumor responses and reducing toxicities.[20] However, whether more selective HDACis will deliver on this premise remains to be determined. Transient depletion of individual HDACs in human tumor cells using small interfering RNA has not conclusively demonstrated whether antitumor actions of broad-acting HDACis can be phenocopied by loss of individual or multiple HDACs.[21-24] Knockdown of HDAC3, and to a lesser extent HDAC1 and 2, resulted in growth inhibition in human colon cancer cell lines; however, the biological response was less potent than vorinostat treatment.[25] Depletion or pharmacological inhibition of HDAC3 triggered apoptosis in cutaneous T-cell lymphoma and multiple myeloma.[21,22] Apoptotic effects in ovarian cancer cell lines following small interfering RNA-mediated knockdown of HDAC2, 4, 8, and 11 have been reported.[23] These studies suggest suppression of a single HDAC may have antitumor effects; however, comprehensive screening approaches using multiple cell systems have not been implemented to date.

Here, we used 3 tractable murine hematological cancer models: MLL-AF9;Nras^{G12D}-driven AML; PML-RARα–driven acute promyelocytic leukemia (APL); and *Myc*-driven B-cell lymphoma (Eμ-*Myc*) to assess the effects of genetically depleting or pharmacologically inhibiting individual HDAC isoforms on tumor cell growth and survival. We demonstrate a unique sensitivity of all 3 malignancies to depletion of *Hdac*3, but no other individual *Hdac*. Furthermore, depletion of both *Hdac*1 with *Hdac*2 induced apoptosis in Eμ-*Myc* lymphoma. These genetic studies were supported by experiments using pharmacological inhibitors of individual or multiple HDAC isoforms that phenocopied the effects of gene knockdown.

Materials

Cell lines

Antibodies to the following proteins were used: HDAC1 (ab7028; Abcam, Cambridge, UK); HDAC2 (ab7029); HDAC3 (ab7030); HDAC6 (no. 2162; Cell Signaling, Danvers, MA; no.); acetylated tubulin (6-11B-1, T7451; Sigma-Aldrich, Castle Hill, Australia); acetylated H4(K5) (no. 9672; Millipore, Arundel, Australia); acetylated H4(K8) (no. 2594; Cell Signaling); acetylated H3(K14) (Millipore, 06-911); p21 (F-5; Santa Cruz, CA); β-actin (Sigma-Aldrich); and HSP90 (ADI-SPA-830; Sapphire Bioscience, Australia). Vorinostat was from Merck (Boston, MA), RGFP966 and RGFP233 from Repligen Corporation (Waltham, MA), Tubacin from Enzo (Sapphire Biosciences), ACY-1215 from Acetylon Pharmaceuticals (Boston, MA); and QVD was from Sigma-Aldrich.

NIH-3T3 and Phoenix cells were cultured in Dulbecco's modified Eagle medium, fetal bovine serum, L-glutamine, and penicillin/streptomycin (Invitrogen, Melbourne, Australia). Eμ-*Myc* lymphoma cells were maintained as previously detailed.[24] MLL-AF9;Nras^{G12D} AML cells were generated as described.[26] APL cells were generated as described.[27] Mouse embryonic fibroblasts (MEFs) were maintained in complete Dulbecco's modified Eagle medium plus β-mercaptoethanol.

RNA interference design

Short hairpin RNA (shRNA)mir30s targeting murine *Hdac* isoforms were designed as previously described (see supplemental Table 1 on the *Blood* Web site).[28-30] Clones were sequence verified using the 5′miR30-ZUBER primer (supplemental Table 3). shRNAs used in APL experiments were generated as described (supplemental Table 2).[28]

Stable transductions of retroviral vectors

Phoenix cells were transfected using calcium phosphate.[28,29] Viral supernatants were spun onto RetroNectin-coated plates (Takara, Clontech) followed by spinfection of tumor cells. APL cells were exposed to concentrated viral supernatants (5× cold PEG-it TM, System Biosciences). Flow cytometry was used to assess transduction efficiency (green fluorescence protein [GFP]/Venus, LSR II, Becton Dickinson).

Proliferation assays

Proliferation was assessed by: (1) competitive proliferation assays as described[26] and percentages of GFP$^+$/Venus$^+$/dsRed$^+$ cells were assessed using flow cytometry; (2) cell counting, whereby cells were plated (5×10^3 cells/well, 24-well plate), counted daily (4 days), replated (5×10^3/well) and recounted (4 days); (3) CellTrace Violet staining (CTV; 1-5 $\times 10^6$ cells, Life Technologies, Mulgrave, Australia), fluorescence-activated cell sorter (FACS)-sorted, serially cultured, and assessed daily by flow cytometry (Canto II, Becton Dickinson); and (4) sorted (GFP$^+$) APL cells (1×10^4 cells/plate) were seeded in methylcellulose medium (MethoCult SF M3434; Stem Cell Technology, Vancouver, Canada), incubated (7-10 days), colonies were scored, pooled, and cells used for immunolabeling, morphologic analysis, and serial replating.

Western blotting and qRT-PCR

Whole cell extracts were prepared and analyzed by western blot as described.[31] RNA was obtained using Qiagen mini kits (Doncaster, Australia) or Trizol (Life Technologies, Mulgrave, Australia), converted to cDNA using M-MLV Reverse transcriptase (RNase H Minus, Point mutant) and random primers (Promega, Madison, WI, USA). SensiFast SYBR green fluorescent nucleic acid stain (Bioline, Alexandria, Australia) was used with quantitative real-time polymerase chain reaction (qRT-PCR) primers described (supplemental Table 3).

Assessment of apoptosis and cell cycle in Eμ-*Myc* cells

Apoptosis was assessed by Annexin V positivity (Becton Dickinson, Australia) with propidium iodide (Sigma-Aldrich) or Fluoro-Gold (Santa Cruz, Dallas, TX) by flow cytometry. Cell cycle was assessed using ClickIt-Edu kit (Life Technologies) as per kit instructions.

Immunophenotyping and morphologic analysis

Flow cytometry was performed on APL cells harvested from methylcellulose. Antibodies used for immunophenotyping were: Ly-6G (Gr-1, no. 25-5931-82; eBioscience, San Diego, CA) and CD11b (MAC1, no. 25-0112-82). Cytospins were stained using the May-Grunwald-Giemsa method (Sigma-Aldrich) and assessed as described elsewhere.[32]

In vivo depletion of *Hdac*3 in AML, Eμ-*Myc* lymphoma, and APL

Tet-on competent MLL-AF9;Nras^{G12D} leukemia cells were transduced (pTRMPV-Neo), G418 selected (1 mg/mL, 6 days), transplanted (1×10^6) into sublethally irradiated (5.5 Gy) recipient mice (CD45.1; shRen.713, n = 12; sh*Hdac*3.987, n = 14), and fed dox (≥day 2). Whole-body bioluminescent imaging was undertaken (day 8, n = 4/group) as described.[33] Bone marrow from leukemic mice was analyzed by flow cytometry for the percentage of Venus$^+$/dsRed$^+$ (shRNA-expressing) cells in donor-derived (CD45.2$^+$) leukemia populations as previously described.[33]

Eμ-*Myc* lymphoma cells (no. 107, CD45.2$^+$) were transduced (pTRMPV-Neo; shScr, sh*Hdac*3.1659, sh*Hdac*3.201), FACS-sorted, inoculated into CD45.1$^+$ mice (5×10^3, n = 12/shRNA); mice were then fed dox (≥day 3). Mice (n = 6/group) were bled (retroorbital), euthanized, and organs removed (day 10); the remainder were euthanized at ethical end points.[34] White blood cells (WBCs; Siemens Advia, Baywater, Australia) and tumor burden (Venus$^+$ cells) were assessed in the peripheral blood (PB) was assessed by flow cytometry.

Transduced APL cells (shLuc or sh*Hdac*3) were FACS-sorted (GFP$^+$) and inoculated (2×10^5 cells/mouse) into 129 SvEv mice (n = 10/cohort) and followed for leukemia development. Genomic DNA from leukemic animals was purified using a QIAamp DNA kit (QIAGEN, Valencia, CA) and PCR performed using primers specific for pRetroSuper (supplemental Table 3).

All in vivo experiments were approved by the animal ethics committees of individual institutes.

Assessment of RGFP966 and RGFP233 in Eμ-*Myc* lymphoma and/or APL in vitro

HDAC3-selective RGFP966 and HDAC1/2-selective RGFP233[35,36] were diluted in dimethylsulfoxide (10 mM) before treatment of Eμ-*Myc* lymphoma or APL cells at concentrations depicted. Apoptosis, cell proliferation, or cell maturity were assessed as described.

Generation of sh*Hdac*3 MEFs

Transgenic mice expressing sh*Hdac*3.1659 or shLuc.1309 were produced as described.[37] MEFs were generated by intercrossing with CAGs-rtTA3 mice[38] and harvesting of E13.5 fetuses. MEFS were plated in 24-well plates (1×10^5/well) and then serially passaged (±dox, 1 μg/mL). Expression of shRNA cassettes was assessed by flow cytometry (Venus$^+$ cells) and target gene knockdown by western blot.

Generation of *Hdac*$^{-/-}$ Eμ-*Myc* lymphoma

Conditional *Hdac*$^{fl/fl}$ mice (Merck) were crossed with Eμ-*Myc*.Mx-Cre mice to generate Eμ-*Myc*.Mx-Cre.*Hdac*$^{fl/fl}$ lymphoma. Tumors were genotyped at end point combined with western blot or qRT-PCR to confirm deletion of individual *Hdacs* (supplemental Figure 7A-B). Eμ-*Myc* tumor cells displaying spontaneous Cre-mediated deletion (see Summers et al[36]) of *Hdac1*, *Hdac2*, or *Hdac6* were used for subsequent experiments and designated Eμ-*Myc.Hdac1*$^{-/-}$, Eμ-*Myc.Hdac2*$^{-/-}$, or Eμ-*Myc.Hdac6*$^{-/-}$.

Statistical analysis

All data including Kaplan-Meier survival curves were analyzed using appropriate statistical tests, including Student *t* test and one-way analysis of variance (ANOVA) with multiple comparisons (GraphPad Prism software). Flow cytometry data were analyzed using FlowJo Analysis software (Treestar). Data are expressed as mean ± standard error of the mean (SEM) and statistical significance assumed at $P < .05$.

Results

Systematic depletion of *Hdac* isoforms in AML, Eμ-*Myc* lymphoma, and APL uncovers sensitivities to depletion of *Hdac*3

We have previously observed potential sensitivities of aggressive MLL-AF9;Nras^{G12D} AML to HDAC inhibition.[26] Here we evaluated this by depleting *Hdac*s 1-11 using independently derived shRNAs and competitive assays to monitor their effects on representation of AML cells in vitro. In contrast to any other single *Hdac*, cells constitutively depleted of *Hdac*3 exhibited reduced representation during 12 days of serial passaging (Figure 1A). *Hdac*3 knockdown efficiency was evaluated by qRT-PCR (day 2) and correlated with the biological effects of depletion (Figure 1B). Validation assays showed dox-inducible depletion of *Hdac*3 caused antiproliferative effects similar to established control shRNAs, including *shMyc.2105*, *shMyb.2652,* and *shMen1.2310* (Figure 1C) that target Myc, Myb, and Menin, respectively.

Next we focused on HDACs inhibited by FDA-approved HDACi, such as vorinostat (HDACs1, 2, 3, and 6) in Eμ-*Myc* lymphoma. An independent set of *Hdac*-directed shRNAs to those used in Figure 1 were validated in NIH-3T3 cells using constitutive (pLMS; supplemental Figure 1) or dox-inducible (pTRMPV-Neo; supplemental Figure 2) vectors by western blot. At least 2 shRNAs effectively depleted each individual *Hdac* and were used in subsequent experiments. Eμ-*Myc* (no. 4242) lymphoma cells were more sensitive to constitutive depletion of *Hdac*3 than to knockdown of *Hdacs1*, *2,* or *6* (Figure 2A-B). Additionally, inducible depletion of *Hdac*3 reproducibly led to the loss of representation of Eμ-*Myc* (no. 4242) cells using multiple shRNAs (Figure 2C-E). A similar loss-of-representation phenotype was observed following knockdown of *Hdac3* in a second Eμ-*Myc* lymphoma (no. 107; supplemental Figure 3A-B).

We recently reported that *Hdac*1 suppressed the development of APL (PML-RAR), but had little role in maintenance of established APL cells.[28] Therefore, we wished to investigate the effects of *Hdac*3 depletion in this malignancy. Using independently derived shRNAs, depletion of *Hdac*3 (Figure 3A-B) significantly reduced the clonogenic potential of APL cells (Figure 3C). Interestingly, morphologic analysis of APL cells showed that *Hdac*3 depletion also induced a more mature cell phenotype (Figure 3Di-ii).

To determine whether *Hdac*3 depletion was detrimental to growth/survival of nontumor cells, we knocked down *Hdac*3 in MEFs. *Hdac*3 depletion had no significant effect on the growth and survival of MEFs up to 13 days following depletion (supplemental Figure 4A; $P > .05$).

Depletion of *Hdac3* induces an antiproliferative response that is not affected by genetic or pharmacological inhibition of apoptosis

After reports suggested that HDAC3 suppression induces tumor cell apoptosis,[21,36] we investigated whether depletion of *Hdac*3 had a pro-apoptotic effect in Eμ-*Myc* cells. No apoptosis induction above background levels was detected in *Hdac*3-depleted cells or cells depleted of any other single *Hdac* isoform (Figure 4A; supplemental Figure 3). In contrast, treatment of Eμ-*Myc* cells with vorinostat mediated a robust apoptotic response, as we had previously observed (Figure 4A).[39] To further demonstrate that induction of apoptosis did not contribute to the loss of cells following knockdown of *Hdac*3, pro-survival *Bcl-2* was overexpressed in Eμ-*Myc* cells (Eμ-*Myc.Bcl-2*; supplemental Figure 3C) because this is reported to prevent vorinostat-mediated apoptosis via the intrinsic apoptotic pathway.[39] *Hdac*3 depletion continued to invoke a loss of representation phenotype in *Bcl-2*–overexpressing cells (Figure 4B-C). Addition of the caspase inhibitor QVD had no effect on suppression of proliferation observed following *Hdac*3 depletion, but QVD did suppress vorinostat-induced apoptosis (Figure 4D). Surprisingly, we did not detect any acute changes in cell cycle following *Hdac*3 depletion using sensitive Edu labeling and pulse chase assays (supplemental Figure 5A). Taken together, these data demonstrate that depletion of *Hdac*3 in Eμ-*Myc* cells does not induce apoptosis or arrest within any specific phase of the cell cycle, and an intact apoptotic response is not required for the antiproliferative effects of *Hdac*3 depletion.

Next we investigated whether depletion of *Hdac*3 affected the proliferative capacity of lymphoma cells. Eμ-*Myc* cells depleted of *Hdac*3 proliferated more slowly than those expressing the control

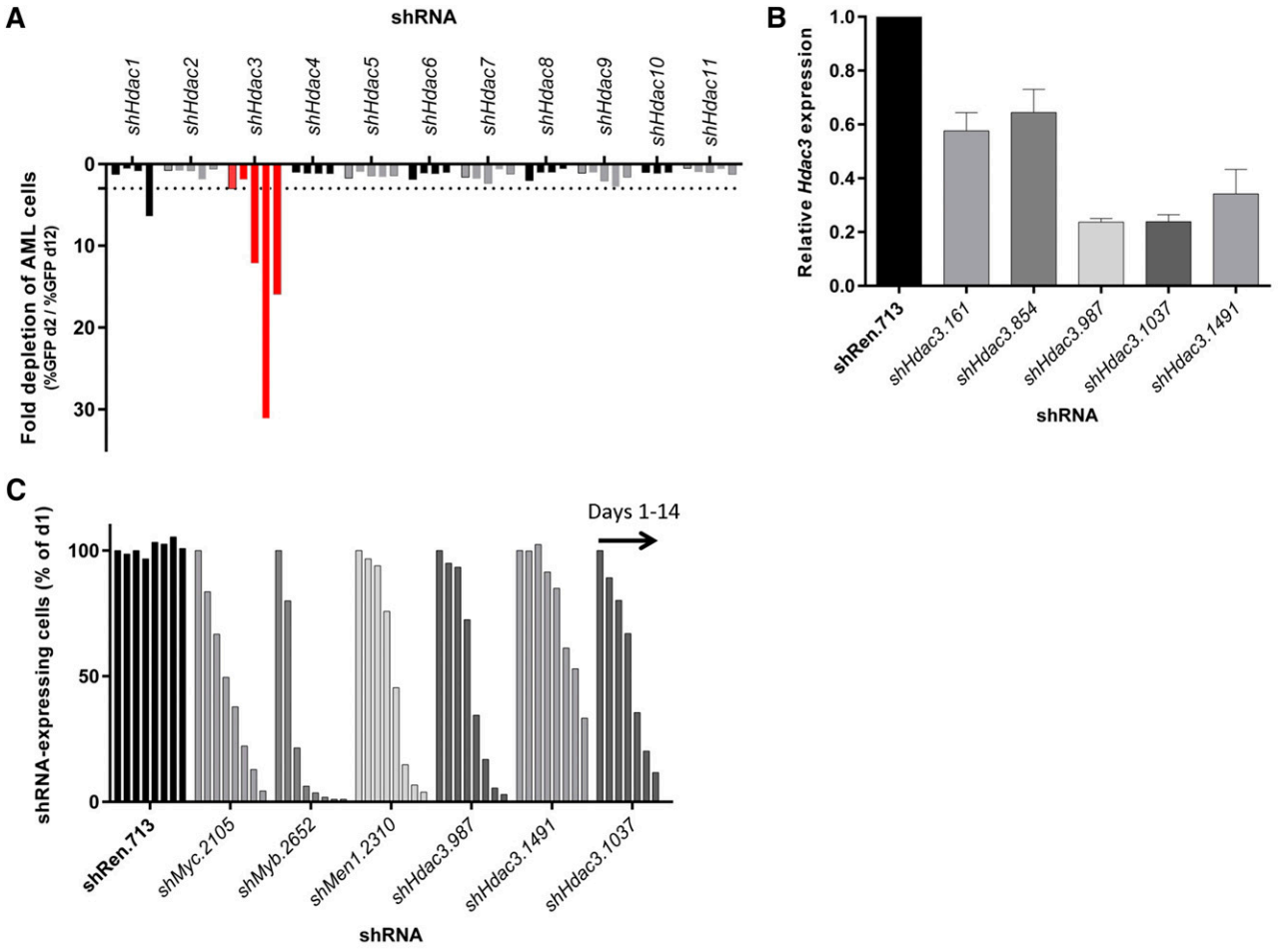

Figure 1. RNAi-mediated screen of all 11 classical *Hdac* isoforms in AML cells (MLL-AF9;Nras^{G12D}) demonstrates a unique dependency on *Hdac*3 expression. Eleven *Hdac* isoforms were depleted in MLL-AF9;Nras^{G12D} AML using multiple shRNAs per *Hdac*. Transduced AML cells (GFP$^+$, shRNA-expressing) were mixed with nontransduced cells and followed for 10 days for cell representation by flow cytometry. (A) Relative depletion of GFP$^+$ AML cells following constitutive (pLMN) depletion of individual *Hdacs* during 10 days of serial culture (*Hdac*3 shown in red). Data are plotted as fold change (GFP% day 2/GFP% day 12). A single experimental screen was undertaken with 4-5 distinct shRNAs per gene represented by individual bars. Dotted line depicts a 3-fold depletion cut off. (B) The efficiency of *Hdac*3 knockdown in AML cells was validated by qRT-PCR (day 2). Results were normalized to glyceraldehyde-3-phosphate dehydrogenase, whereas relative messenger RNA level in control cells (shRen.713) was set to 1 (n = 3-4 independent biological replicates). Data are presented as mean ± SEM. (C) Dox-inducible depletion of *Hdac*3 in AML. Each series of bars demonstrates a time course: days 1, 2, 4, 6, 8, 10, 12, and 14. The percentage of shRNA- expressing cells (Venus$^+$/dsRed$^+$) was normalized to day 1. Data are representative of a single experiment using 3 individual shRNAs to *Hdac3* (*shHdac3.987*, *shHdac3.1491*, *shHdac3.1037*). Established control shRNAs to *Myc*, *Myb*, and MLL/AF9 cofactor *Men1* were included for comparison.

shRNA (Figure 4E). In addition, cell counting/replating assays conclusively showed that the proliferation of Eμ-*Myc* lymphoma was significantly attenuated when *Hdac*3 was depleted (Figure 4F). Assessment of cell populations at the experiment's end demonstrated outgrowth of GFP$^-$ cells not expressing sh*Hdac*3, suggesting selection of cells without *Hdac*3 depletion (Figure 4G). Overall, our results suggest that depletion of *Hdac*3 in Eμ-*Myc* lymphoma leads to a loss of proliferation phenotype that is independent of apoptosis.

Loss of p21$^{WAF1/CIP1}$ does not affect the antiproliferative response mediated by *Hdac*3 depletion

Previous investigators have reported changes to the expression of various cell-cycle/checkpoint proteins, including p15^{INK4b},[40] p21$^{WAF1/CIP1}$,[21,40] p27,[41] p53,[41,42] p57,[43] and/or Rb[44,45] following *Hdac*3 depletion. Therefore, we probed for the expression of all mentioned cell-cycle regulatory proteins in *Hdac*3-depleted Eμ-*Myc* cells by western blot (data not shown). Interestingly, only p21$^{WAF1/CIP1}$ was reproducibly upregulated in a time-dependent manner, such that potent sh*Hdac*3.1659 increased p21$^{WAF1/CIP1}$ levels by day 3, whereas the less potent sh*Hdac*3.201 increased p21$^{WAF1/CIP1}$ expression at day 6 (supplemental Figure 5B). Assessment of *Cdkn1a* expression by qRT-PCR demonstrated that depletion of *Hdac*3 had no effect on the transcription of *Cdkn1a*, suggesting posttranslational regulation/stabilization of p21$^{WAF1/CIP1}$ (supplemental Figure 5C). Genetic deletion of *Cdkn1a* (Eμ-*Myc*.*Cdkn1a*$^{-/-}$) did not prevent the antiproliferative effects observed following *Hdac*3 depletion (Figure 4H; supplemental Figure 5D). These results suggest that p21$^{WAF1/CIP1}$ regulation/stabilization did not mediate the growth suppressive effects of *Hdac*3 depletion.

In vivo *Hdac*3 depletion reduces tumor burden and/or significantly extends the survival of mice bearing AML, Eμ-*Myc* lymphoma, or APL cells

Our in vitro studies reproducibly demonstrated that *Hdac*3 depletion reduced the proliferation of AML, Eμ-*Myc* lymphoma, and APL cells; we sought to confirm this in vivo. We inoculated CD45.1$^+$ congenic C57BL/6 mice with luciferase-expressing AML cells transduced with dox-inducible sh*Hdac*3.987 (n = 14) or nontargeting shRen.713 (n = 12) and initiated *Hdac*3 depletion 2 days after transplantation. Remarkably, in vivo depletion of *Hdac*3 significantly reduced tumor

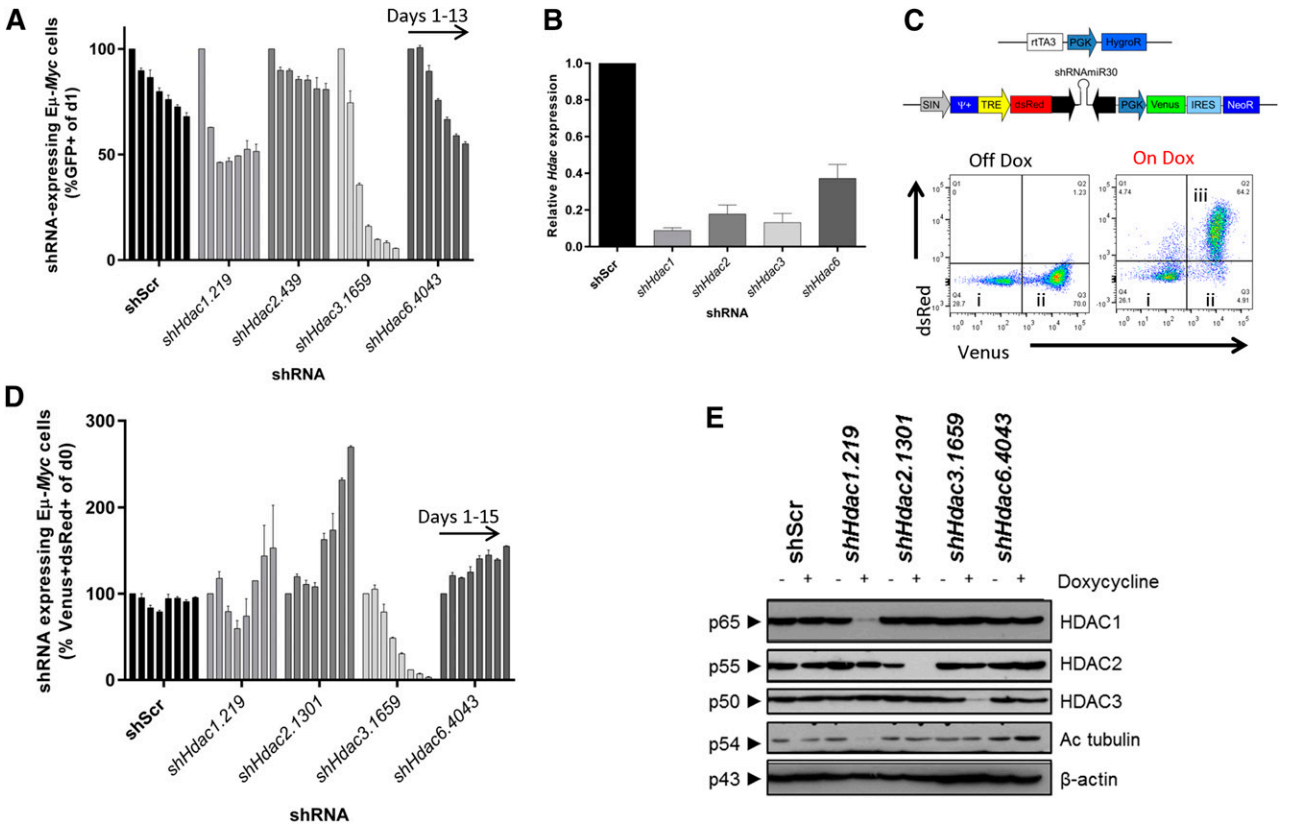

Figure 2. Systematic shRNA-mediated screen of individual *Hdac* isoforms uncovers sensitivity of Eμ-*Myc* lymphoma cells to depletion of *Hdac*3. Eμ-*Myc* lymphoma cells (no. 4242) were transduced with constitutive (pLMS) or dox-inducible (pTRMPV-Neo) retroviral vectors expressing shRNAs targeting HDACs1, 2, 3, or 6. Cells were isolated by FACS and then serially passaged (±dox) for up to 15 days. The percentage of shRNA-expressing cells (GFP$^+$, pLMS; or Venus$^+$/dsRed$^+$, pTRMPV-Neo) were assessed by flow cytometry (days 1, 3, 5, 7, 9, 11, 13) and data were normalized to day 1, as depicted. (A) Constitutive depletion of individual *Hdacs* in Eμ-*Myc* cells in vitro (n = 2 biological replicates). Data are presented as mean ± SEM. (B) qRT-PCR was used to determine the efficiency of *Hdac* depletion in Eμ-*Myc* cells (day 3). Results were normalized to L32, whereas relative mRNA level in control cells (shScr) was set to 1 (n = 3-4 biological replicates). Data are presented as mean ± SEM. (C) Schematic representation of the dox-inducible vector system (pTRMPV-Neo). Representative dot plots demonstrating: (i) nontransduced (Venus$^-$) cells; (ii) transduced (Venus$^+$) cells; and (iii) shScr-expressing (Venus$^+$/dsRed$^+$) Eμ-*Myc* cells from at least 3 independent experiments. (D) Dox-inducible depletion of individual *Hdacs* in Eμ-*Myc* tumor cells in vitro (no. 4242; n = 2 independent experiments; days 1, 3, 5, 7, 9, 11, 13, 15). Data are presented as mean ± SEM. (E) Western blotting was used to demonstrate the efficiency of inducible *Hdac* depletion in Eμ-*Myc* cells (day 3). Hyperacetylated tubulin (Ac tubulin) was used as a surrogate readout for *Hdac*6 depletion, whereas changes to its levels in non-sh*Hdac*6 samples represent background variability (for example sh*Hdac*1). A representative experiment from 3 biological replicates is shown. Molecular weights of individual proteins are to the left of each blot.

burden (Figure 5A) and provided significant survival benefit in mice bearing AML (Figure 5B). At the terminal disease stage, bone marrow of control mice predominantly showed shRen.713-expressing cells (Venus$^+$/dsRed$^+$), whereas recipients of sh*Hdac*3.987-expressing cells showed an outgrowth of AML cells that had evaded shRNA expression (CD45.2$^+$/ Venus$^+$/dsRed$^-$; Figure 5C; supplemental Figure 6A), indicating a strong selection against effective *Hdac*3 suppression.[34]

We next transplanted Eμ-*Myc* lymphoma (no. 107) transduced with dox-inducible shScr, sh*Hdac*3.1659, or sh*Hdac*3.201 into CD45.1$^+$ congenic C57BL/6 mice (n = 36) and allowed engraftment before dox treatment (day 3). In vivo depletion of *Hdac*3 significantly reduced WBC count (Figure 5E), the percentage of Venus$^+$ tumor cells in PB (Figure 5F), and spleen weight (Figure 5G). Consistent with the data from the AML system, we observed outgrowth of nontransduced Eμ-*Myc* cells (Venus$^-$; supplemental Figure 6B) in mice at ethical end points preventing any survival advantage (data not shown).

We then knocked down *Hdac*3 (or control Luc) in frankly leukemic APL cells. Sorted GFP$^+$ APL cells were transplanted into 129 SvEv recipient mice and engraftment followed by analysis of PB. Inoculation of GFP$^+$/sh*Hdac*3 APL cells resulted in no, or very few, GFP$^+$ cells detected in PB samples, whereas control cells grew exponentially (data not shown). Although all control mice (n = 10) developed APL and were euthanized by 50 days after transplantation, 7 of 10 GFP$^+$/sh*Hdac*3 mice remained disease-free for >300 days, whereas the remaining 3 of 10 GFP$^+$/sh*Hdac*3 mice developed APL (supplemental Figure 6C). In these mice, APL cells resident at the end of the experiment showed WT *Hdac*3 expression, suggesting selection against *Hdac*3 depletion (supplemental Figure 6D). Additionally, PCR analysis from genomic DNA extracted from spleens of 2 leukemic mice confirmed that the leukemic cells originated from nontransduced cells that are present in small numbers (<1%) upon sorting because we were unable to amplify a DNA fragment corresponding to the vector used to transduce cells that should have been stably integrated into the host genome (supplemental Figure 6E).

HDAC3-selective RGFP966 reproduces *Hdac3* depletion in Eμ-*Myc* lymphoma and APL

Next we asked whether the biological effects of *Hdac*3 depletion could be phenocopied pharmacologically with the HDAC3-selective inhibitor, RGFP966.[22,35] Eμ-*Myc* lymphoma cells did not undergo apoptosis following incubation with RGFP966 (≤1 μM, 48 hours; Figure 6A) but proliferated significantly more slowly than vehicle-treated controls in the presence or absence of pro-survival BCL-2 overexpression (Figure 6B), confirming our genetic depletion studies

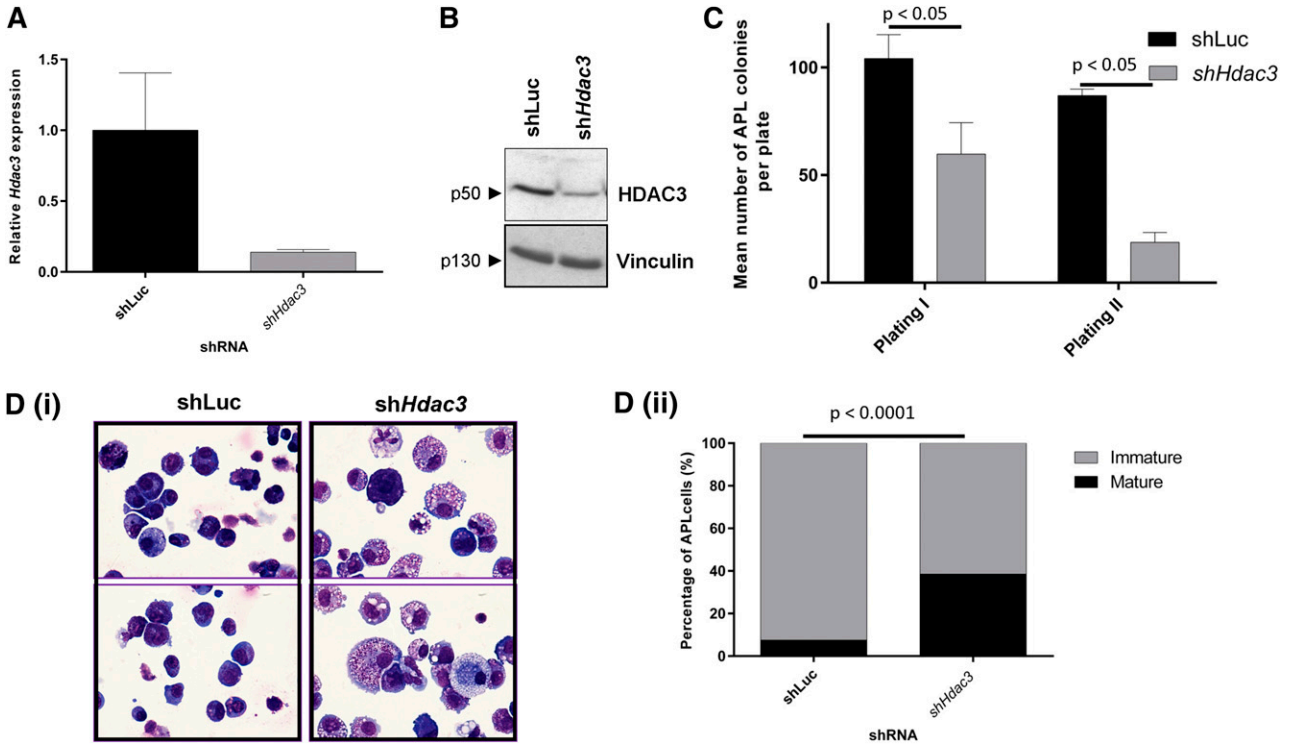

Figure 3. In vitro depletion of *Hdac*3 reduces growth and triggers differentiation in established APL cells. APL blasts from 129*SvEv* mice were transduced with constitutive pRetroSuper vectors expressing sh*Hdac*3 or control shLuc and sorted for GFP positivity, then assessed for (A) depletion of *Hdac3* by qRT-PCR. Values are normalized against glyceraldehyde-3-phosphate dehydrogenase and referred to CTRL (shLuc) (n = 2 biological replicates). Data are presented as mean ± SEM. (B) Depletion of HDAC3 by western blot; Vinculin was used as a loading control. Molecular weights of individual proteins are to the left of each blot. (C) Loss of clonogenicity by serial replating assay (data are presented as mean number of colonies counted 7-10 days after seeding 1×10^4 leukemic cells ± SEM (n = 3 independent experiments). Data are presented as mean ± SEM. Statistical analysis was performed with a paired *t* test. (D) Differentiation by morphologic analysis of the GFP^+/APL cells, harvested after plating in methylcellulose medium (first methylcellulose): (i) representative cytospins; (ii) percentage of mature and immature cells (×60 magnification, May Grünwald-Giemsa staining, Olympus BX51). The prevalence of mature and immature cells was analyzed morphologically in cytological slides and the absolute percentage of mature cells was reported. Experiments were repeated 3 times (biological triplicate). At least 300 cells were scanned for each case. Statistical analysis was performed with the Fisher exact test.

(see supplemental Figure 7A for biomarker studies). Similarly, RGFP966 did not induce apoptosis in APL cells (supplemental Figure 7B; ≤1 μM) but did reduce clonogenicity and increased maturation (Figure 6C-F). Treatment of wild-type hematopoietic progenitor cells with RGFP966 had only minor effects on cell clonogenicity (data not shown).

A pro-apoptotic effect requires the depletion of *Hdac*1 and *Hdac*2 in Eμ-*Myc* lymphoma

We next exploited our ability to delete/deplete multiple *Hdac*s to determine whether loss of more than a single *Hdac* isoform could induce a pro-apoptotic response. Here we deleted *Hdac1*, *Hdac2*, or *Hdac6* (supplemental Figure 8A-C) combined with knockdown of *Hdac*1, *Hdac*2, *Hdac*3, or *Hdac*6 in Eμ-*Myc* lymphoma. Combined deletion/depletion of *Hdac1* with *Hdac*2 rapidly reduced the representation of Eμ-*Myc* cells to a greater extent than single isoform depletion experiments. *Hdac*6 knockdown had no effect, whereas the antiproliferative effect of *Hdac*3 depletion was not further potentiated by *Hdac1* deletion (Figure 7A) or *Hdac2* deletion (data not shown). Reciprocal knockout of *Hdac2* combined with *Hdac1* depletion confirmed this response (supplemental Figure 8D-F). We then depleted *Hdac*s1-3 in Eμ-*Myc.Hdac6*$^{-/-}$ lymphoma and observed that only combined depletion of *Hdac6* with *Hdac*3 reduced the representation of tumor cells (Figure 7B). However, the antiproliferative effects of combined *Hdac*3 with *Hdac*6 depletion/deletion were not greater than those observed following *Hdac*3 depletion alone.

We then investigated whether the effects of suppressing *Hdac*1 with *Hdac*2 were due to induction of apoptosis and whether this genetic effect could be phenocopied pharmacologically. The most profound biological response to deleting/depleting *Hdac*1 with *Hdac*2 in Eμ-*Myc* lymphoma was apoptosis (Figure 7C; supplemental Figure 8E-F). Moreover, treatment of Eμ-*Myc* lymphoma with the HDAC1/2 inhibitor RGFP233[22] phenocopied the effects observed following genetic deletion/depletion of *Hdac1* with *Hdac2* (Figure 7D).

To validate the effects of genetically deleting/depleting *Hdac*1 with *Hdac*2 in vivo, we transplanted Eμ-*Myc.Hdac1*$^{-/-}$ cells transduced with dox-inducible vector pTRMPVIR[34] expressing sh*Hdac*2.439 or shScr into NSG mice (n = 32). Tumor-bearing mice were fed dox (day 3) and assessed for tumor burden by flow cytometry (days 16, 17, and/or 22; supplemental Figure 8G). Strikingly, combined deletion/depletion of both *Hdac1* with *Hdac*2 significantly reduced tumor burden ($Venus^+$/$dsRed^+$ cells) in the PB (days 16 and 22; supplemental Figure 8H), spleen (day 17; supplemental Figure 8I), and bone marrow (day 17; supplemental Figure 8J). The outgrowth of $Venus^+$/$dsRed^-$ cells was observed in mice bearing Eμ-*Myc.Hdac1*$^{-/-}$ lymphoma, suggesting a selection against *Hdac*2 depletion (supplemental Figure 8K).

Discussion

Broad clinical use of HDACi targeting multiple HDAC isoforms (vorinostat, belinostat, panobinostat, romidepsin) has been hampered

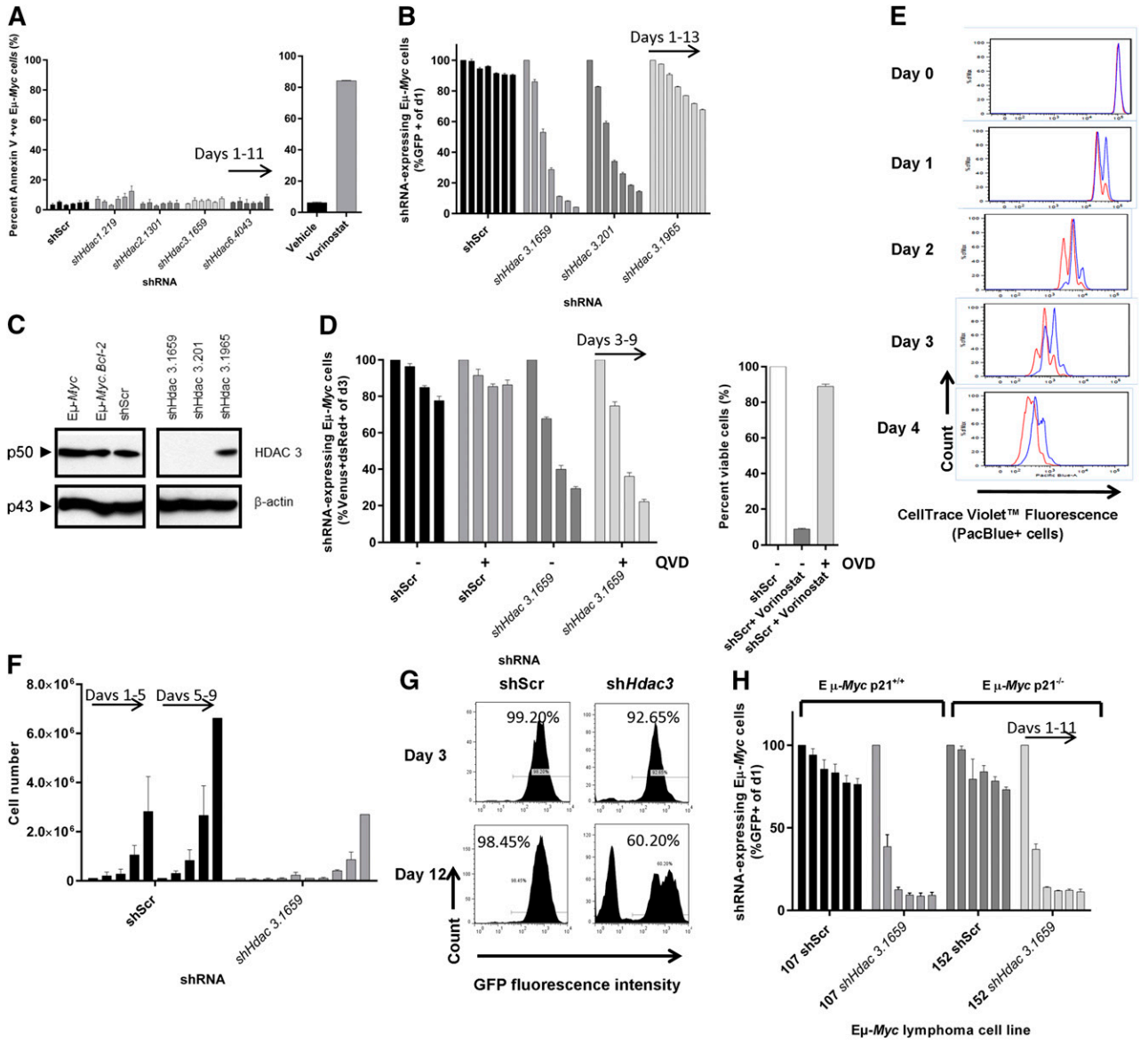

Figure 4. Depletion of *Hdac3* in Eμ-*Myc* lymphoma induces an antiproliferative response that is not affected by genetic or pharmacological apoptosis inhibitors or by loss of p21$^{WAF1/CIP1}$. Eμ-*Myc* lymphoma cells were transduced with pTRMPV-Neo vectors expressing sh*Hdac3* or control shScr cassettes, isolated by FACS (100% GFP$^+$), serially passaged (±dox) for up to 15 days. (A) The induction of apoptosis was assessed by phosphatidylserine externalization (Annexin V$^+$) using flow cytometry. As a positive control, we treated Eμ-*Myc* lymphoma cells with vorinostat (24 hours, 1 μM). Data are presented as percentage of Annexin V positive cells (mean ± SEM, n = 2 biological replicates). Individual bars demonstrate day of analysis (days 1, 3, 5, 7, 9, 11). (B-C) Eμ-*Myc* lymphoma cells (no. 107) were stably transduced with pMSCV.*Bcl-2*-mCherry to overexpress pro-survival *Bcl-2*. Eμ-*Myc.Bcl-2* lymphoma cells were then transduced with constitutive vectors expressing shRNAs against *Hdac3* or shScr, serially passaged, and assessed by (B) competitive proliferation assay where the percentage of GFP$^+$ cells were normalized to day 1 and individual bars represent days of analysis (days 1, 3, 5, 7, 9, 11, 13; 3 individual shRNAs were tested; 2 biological replicates) and (C) HDAC3 depletion was confirmed by western blot. A representative experiment from 3 biological replicates is shown. Molecular weights of individual proteins are to the left of the blot. (D) Caspase activation was inhibited by treating Eμ-*Myc* lymphoma cells expressing dox-inducible shRNAs with pan-caspase inhibitor QVD (10 μM, n = 3 biological replicates); cell growth was assessed using competitive proliferation assays (±dox). Data are presented as mean percentage of shRNA-expressing cells (Venus$^+$/dsRed$^+$, dox-treated only, days 3, 5, 7, 9) and normalized to day 3 ± SEM. The activity of QVD was confirmed in Eμ-*Myc* cells treated with vorinostat (1 μM) ± QVD (presented as percentage viable cells). The proliferation of Eμ-*Myc* cells depleted of *Hdac3* was measured using a carboxyfluorescein diacetate succinimidyl ester–like assay (CTV) and by cell counting/replating assays. (E) Eμ-*Myc* cells (no. 107) were transduced with constitutive (pLMS) vectors expressing sh*Hdac3*.1659 or shScr, immediately stained with CTV, allowed to expand in culture overnight, and then FACS-sorted to a single population of GFP$^+$/CTV$^+$ (PacBlue$^+$) cells. Cells were serially cultured for up to 5 days and underwent daily assessment of their proliferative capacity by flow cytometry (ie, loss of CTV cells over time; shScr, red line; *shHdac3*, blue line). Individual plots represent daily flow cytometry analysis and are representative of 3 individual biological experiments. (F) Eμ-*Myc* lymphoma cells constitutively depleted of *Hdac3* were seeded (5 × 10^3 cells; day 1) into 24-well plates (shScr vs sh*Hdac3*) followed by daily cell counts (individual bars represent days 1, 2, 3, 4, 5), then replated (5× 10^3 cells; day 5) and counted daily (n = 3 biological replicates; bars represent days 5, 6, 7, 8, 9). Data are presented as mean ± SEM. (G) Representative histograms demonstrate the percentages of shRNA-expressing (GFP$^+$) Eμ-*Myc* cells on days 3 and 12 of cell counting/replating assay. (H) Eμ-*Myc.Cdkn1a*$^{+/+}$ (no. 107) or Eμ-*Myc.Cdkn1a*$^{-/-}$ (no. 152) lymphoma cells were depleted of *Hdac3* and cell proliferation was assessed by competitive proliferation assay. Individual bars represent percentages of shRNA-expressing (GFP$^+$) Eμ-*Myc* cells normalized to day 1 (n = 3 biological replicates; individual bars represent days 1, 3, 5, 7, 9, 11). Data are presented as mean ± SEM.

by dose limiting toxicities. Here we investigated whether RNA interference (RNAi)-mediated depletion of a single *Hdac* was capable of reproducing the anti-proliferative or pro-apoptotic effects of broader spectrum HDACi in 3 murine models of hematological neoplasms: 2 AMLs (MLL-AF9;Nras^{G12D} and PML-RARα APL) and Eμ-*Myc* B-cell lymphoma. Strikingly, we demonstrated that depletion of *Hdac3* consistently attenuated tumor cell proliferation in each tumor model tested in the absence of an apoptotic effect. Additionally, combined

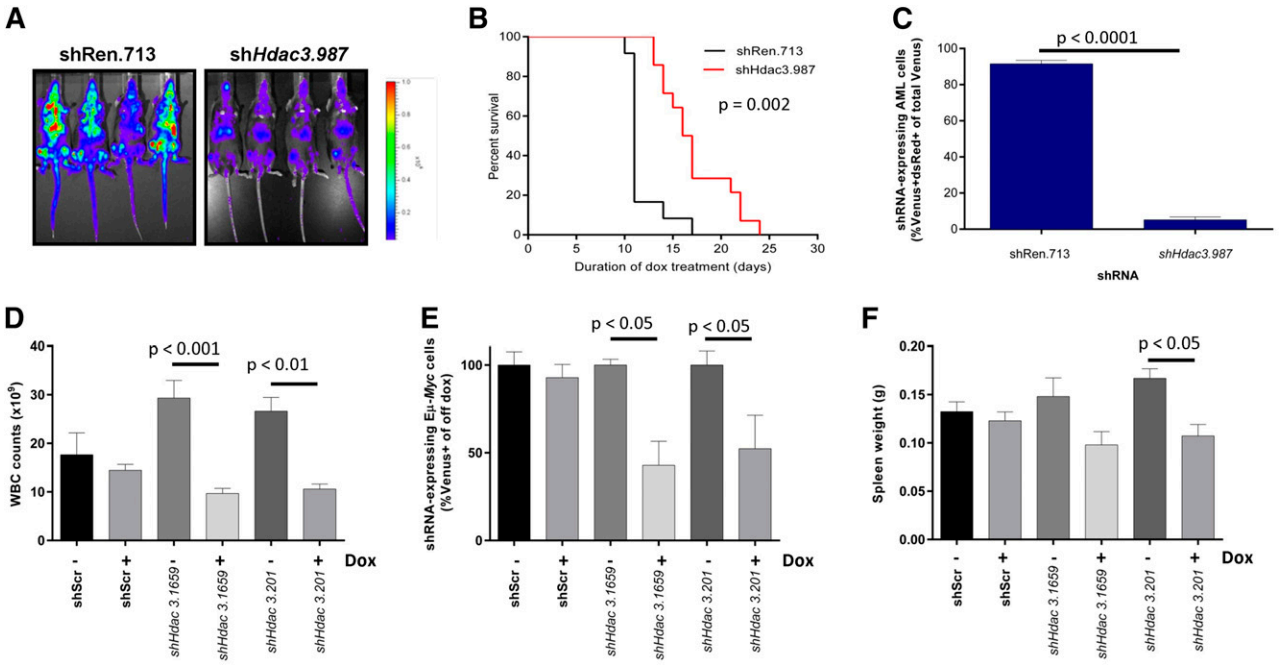

Figure 5. In vivo *Hdac*3 depletion reduces tumor burden and/or significantly extends the survival of mice bearing AML or Eμ-*Myc* lymphoma. MLL-AF9;$Nras^{G12D}$ AML cells transduced with dox-inducible shRNA constructs (pTRMPV-Neo) were transplanted into $CD45.1^+$ mice and shRNA expression was induced 2 days after tumor inoculation by addition of dox to food and drinking water (shRen.713, n = 14; sh*Hdac3.987*, n = 12). (A) Tumor burden was assessed by bioluminescent imaging following 8 days of dox treatment. (B) Kaplan-Meier curves for survival analysis of mice bearing transplanted AML tumor with indicated pTRMPV-Neo constructs. Day 0 denotes the beginning of dox treatment. Statistical analysis was undertaken using a log-rank (Mantel-Cox) test. (C) Percentage of shRNA-expressing ($Venus^+$/$dsRed^+$) tumor cells in the bone marrow remaining at terminal disease stage were analyzed using a Student *t* test ($P < .0001$). Eμ-*Myc* tumor cells (no. 107) were transduced with dox-inducible pTRMPV-Neo with shRNA cassettes targeting *Hdac*3 (sh*Hdac*3.1659, n = 12; sh*Hdac*3.201, n = 12) or shScr control (n = 12), FACS-sorted, and transplanted into $CD45.1^+$ mice (5×10^3 cells per mouse). On day 3 postinoculation, mice (n = 6/group) were fed dox in food and water to initiate expression of shRNAs in vivo. Mice were bled and sacrificed on day 10 to assess (D) WBC count, (E) percentage of tumor cells ($Venus^+$) in PB by flow cytometry, and (F) spleen size in mice bearing Eμ-*Myc* lymphoma. Data are presented as mean ± SEM. Two biological experiments were undertaken. Data were analyzed using one-way ANOVAs and appropriate post-hoc tests.

deletion/depletion of *Hdac*1 with *Hdac*2 was sufficient to induce a pro-apoptotic response in Eμ-*Myc* lymphoma suggesting that HDACis in development should target HDAC3 alone or both HDAC1 and HDAC2.

Using RNAi technology[34,37,46] and an unbiased screening approach, we uncovered unique dependencies of established AML, Eμ-*Myc* lymphoma, and APL to *Hdac*3 expression in vitro and in vivo. However, in contrast to a recent report that *Hdac*3 suppression induces apoptosis in multiple myeloma cells,[21] we were unable to detect any significant level of apoptosis following *Hdac*3 depletion in Eμ-*Myc* lymphoma. Indeed, loss of *Hdac*3 in Eμ-*Myc* tumor cells led to an antiproliferative response that was not attenuated by overexpression of pro-survival BCL-2 or pharmacological inhibition of pro-apoptotic caspases. In agreement, the HDAC3-selective compound RGFP966 mediated an antiproliferative response.

Intriguingly, we were unable to detect acute changes to the cell cycle using sensitive, Edu-based DNA labeling assays. This is consistent with reports demonstrating reduced proliferation of human lung fibroblasts following depletion of ribosomal proteins RP5/RP11[47] and delayed tumor growth in Eμ-*Myc* mice hypomorphic for RPL24[48] that could not be attributed to cell-cycle arrest but likely is due to reduced ribosomal content and rates of translation.

Cyclin-dependent kinase inhibitor $p21^{Cip1/Waf1}$ was upregulated following *Hdac*3 depletion in Eμ-*Myc* lymphoma, as observed by others.[25,49] In contrast to reports that the antitumor effects of HDACi can be mediated in part by $p21^{Cip1/Waf1}$,[50-52] knockout of *Cdkn1a* (Eμ-*Myc*.$Cdkn1a^{-/-}$) did not attenuate the loss of proliferation phenotype observed following *Hdac*3 depletion. This is in agreement with our previous report that deletion of *Cdkn1a* in Eμ-*Myc* lymphoma did not alter sensitivity to vorinostat-induced cell death or prevent cell-cycle arrest.[24]

Although all 3 leukemias/lymphomas demonstrated significant antiproliferative effects following *Hdac*3 depletion in vitro and in vivo, *Hdac*3 depletion in APL cells also triggered differentiation and led to a more mature phenotype. Furthermore, low concentrations of RGFP966 were able to mimic *Hdac*3 depletion by reducing clonogenicity and upregulating the myeloid differentiation markers Gr.1 and CD11b (MAC1) concomitant with morphological changes reminiscent of differentiated myeloid cells.[28] This suggests that low-dose HDAC3-selective inhibition in patients with APL may promote tumor cell differentiation and enable tumor remissions without the need for toxic chemotherapy, similar to that observed with ATRA or arsenic trioxide.[27,53,54]

Our data also provide clear genetic evidence that isoform-selective inhibitors targeting alternative HDACs, including HDAC6, may not provide potent antitumor effects. Recent reports highlighted HDAC6 as a key target of broad-acting HDACi [55-57]; however, our data demonstrate that genetic depletion/deletion of *Hdac*6 had only minor, if any, growth inhibitory effects in AML or Eμ-*Myc* lymphoma. In agreement, suppression of HDAC6 did not elicit growth inhibition in Burkitt lymphoma,[58] lung carcinoma,[59] oncogenic Bcr-Abl–addicted myeloid cells,[29] or neuroblastoma.[60] Therefore, our data do not support the development and use of HDAC6-selective inhibitors in patients with hematological malignancies modeled in our preclinical studies.

Because depletion of *Hdac*3 alone was unable to induce apoptosis, we investigated whether deletion of 1 *Hdac* isoform is able to cooperate with depletion of another *Hdac* to induce a pro-apoptotic response. By genetically deleting *Hdac1*, *Hdac2*, or *Hdac6* in Eμ-*Myc* lymphoma

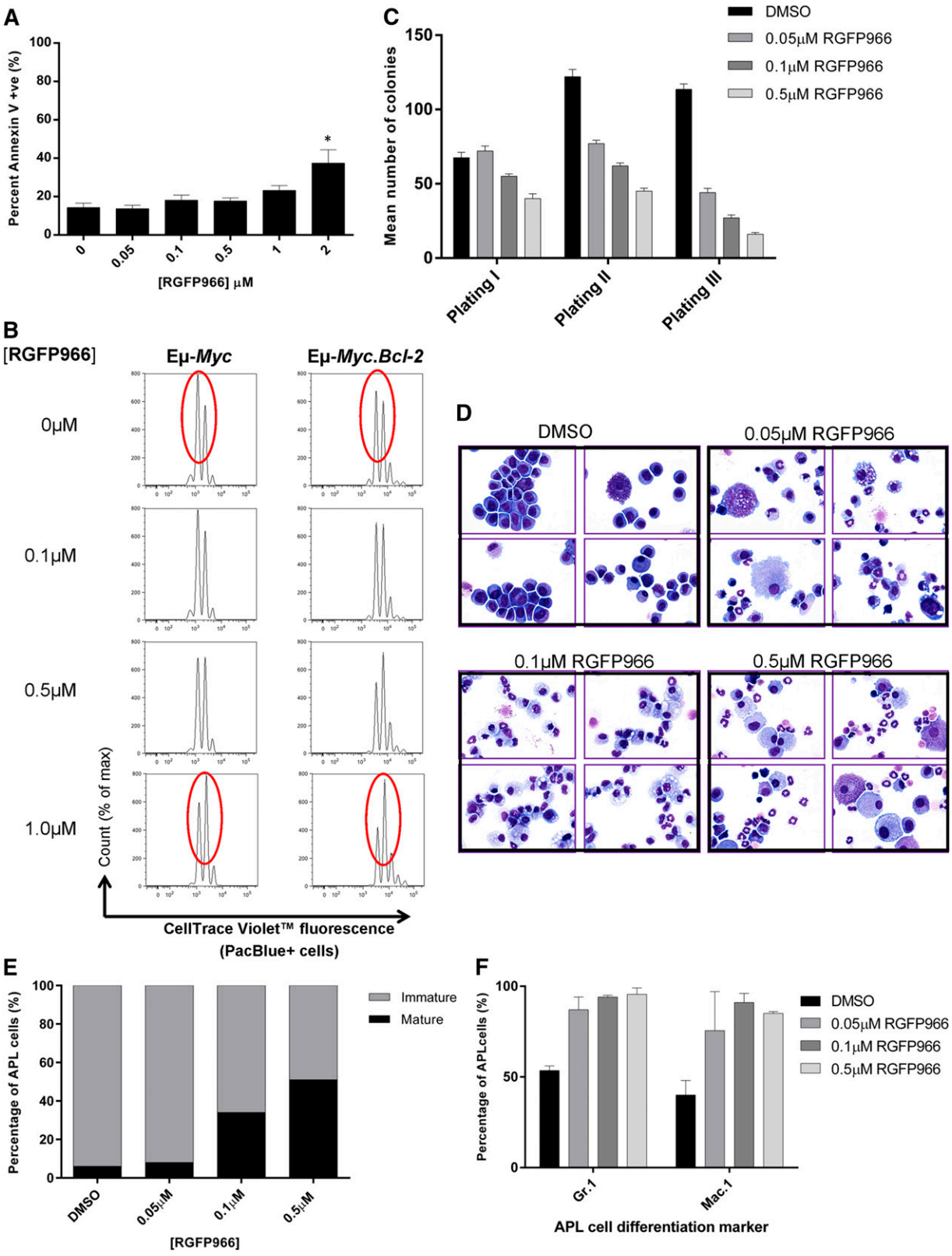

Figure 6. Treatment of Eμ-*Myc* lymphoma or APL cells with HDAC3-selective RGFP966 mimics HDAC3 depletion. Eμ-*Myc* lymphoma and APL cells were treated with low micromolar concentrations of RGFP966 (≤2 μM) in vitro and assessed for apoptosis and cell proliferation. (A) Assessment of apoptosis (Annexin V/PI) in Eμ-*Myc* cells (no. 107) after 48 hours of treatment with RGFP966 using flow cytometry (n = 3 biological replicates; $^*P < .05$). Data were analyzed using a one-way ANOVA. (B) Proliferation of Eμ-*Myc* (no. 107, n = 3 biological replicates) and Eμ-*Myc.Bcl-2* (n = 2 biological replicates) cells was assessed using CTV staining following RGFP966 treatment (≤1 μM, 48 hours). Cells were analyzed for cell division and measured as discrete peaks of decreasing CTV fluorescence (PacBlue$^+$ cells) using flow cytometry. Red ovals highlight the CTV peaks that demonstrate anti-proliferative effects of RGFP966. (C) APL cells were treated with RGFP966 at the indicated concentrations and subjected to colony-forming assays whereby cells were plated in methylcellulose (1 × 104 cells), left for 7-10 days, counted, and replated. Serial replating of RGFP966-treated APL cells led to a dose-dependent reduction in colony forming potential. Data are presented as mean number of colonies counted after 7-10 days ± SEM from 3 biological replicates. (D) Histological assessment of APL cell maturity

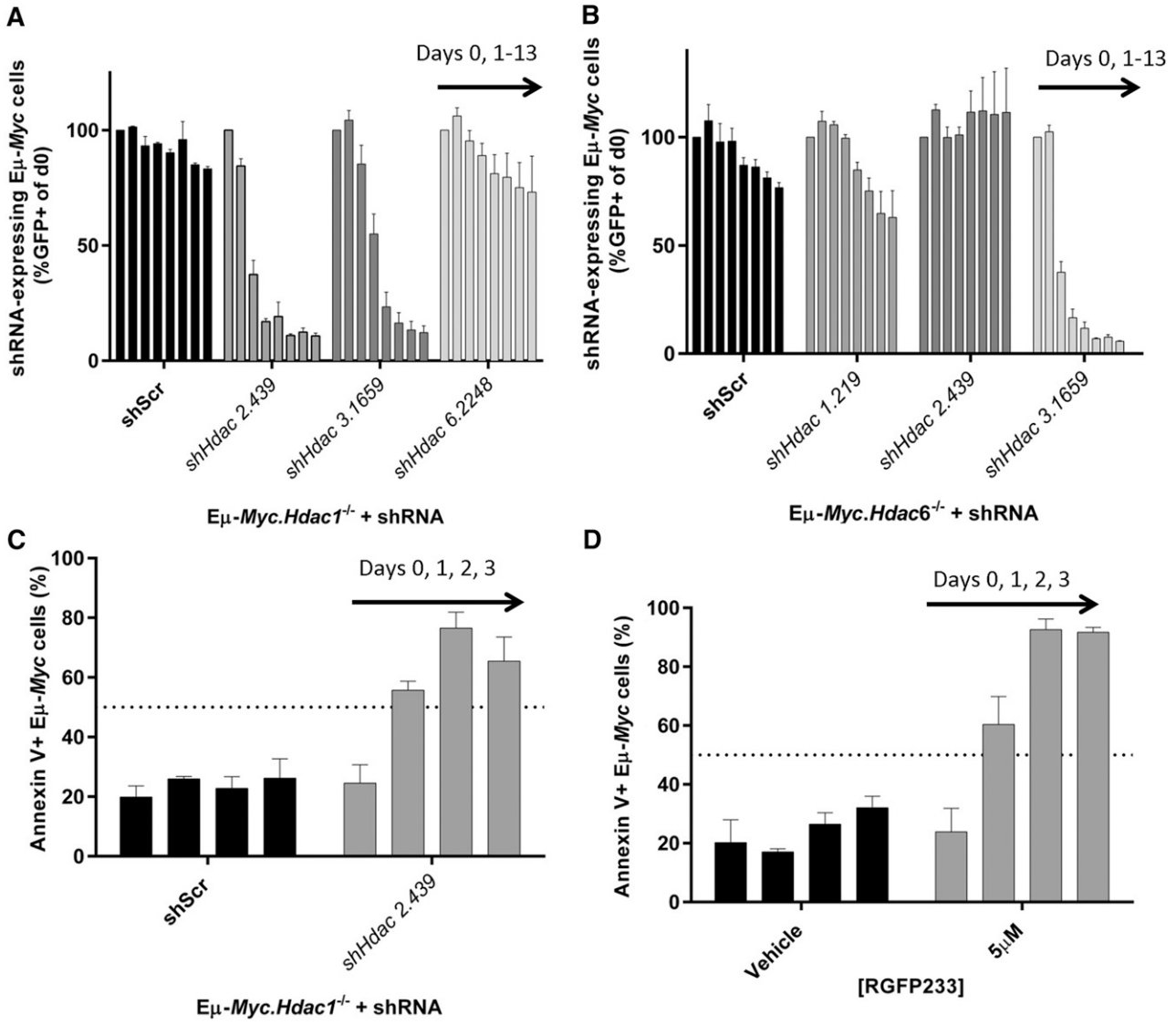

Figure 7. A pro-apoptotic effect requires the depletion of *Hdac1* and *Hdac2* in Eμ-*Myc* lymphoma. We produced tractable Eμ-*Myc* lymphoma cells with conditional knockout of *Hdac1*, *Hdac2*, or *Hdac6* (Eμ-*Myc.Hdac1*$^{-/-}$; Eμ-*Myc.Hdac2*$^{-/-}$; Eμ-*Myc.Hdac6*$^{-/-}$) and transduced these with shRNAs against *Hdac1, Hdac2, Hdac3*, or *Hdac6*. (A) Eμ-*Myc.Hdac1*$^{-/-}$ lymphoma was transduced with constitutive (pLMS) vectors containing shRNA cassettes against *Hdac*2, *Hdac*3, or *Hdac*6, FACS-sorted to approximately 50% GFP^{+}, and 50% GFP^{-}, and cell representation followed over time using competitive proliferation assays, as described previously. Individual bars represent daily flow cytometry assessment of GFP positive cells (days 0, 1, 3, 5, 7, 9, 11, 13) from 3 independent replicates (mean ± SEM) and normalized to day 0. (B) Effects of constitutively depleting *Hdac*1, *Hdac*2, or *Hdac*3 in Eμ-*Myc.Hdac6*$^{-/-}$ cells using competitive assays. Each bar represents different days of testing: days 0, 1, 3, 5, 7, 9, 11, 13. Data are presented as mean ± SEM of 3 biological replicates. (C) Eμ-*Myc.Hdac1*$^{-/-}$ cells transduced with sh*Hdac*2.439 were FACS-sorted (GFP^{+}) immediately following transduction and assessed for the induction of apoptosis by Annexin/propidium iodide staining using flow cytometry. Individual bars represent daily mean percentages of Annexin V–positive cells (days 0, 1, 2, 3) ± SEM (3 biological replicates). (D) Eμ-*Myc* lymphoma cells (no. 107) were treated with HDAC1/2-selective RGFP233 (5 μM) and assessed for apoptosis (Annexin/propidium iodide) by flow cytometry at indicated time points. Data are presented as mean ± SEM (3 biological replicates).

and concomitantly knocking down alternative *Hdac*s, we uncovered a functional interaction between *Hdac*1 and *Hdac*2. Importantly, we observed that suppression of both *Hdac*1 with *Hdac*2 was pro-apoptotic in Eμ-*Myc* lymphoma. This is not surprising considering the functional redundancy reported between these 2 *Hdac* isoforms.[61,62] Pharmacological validation using the HDAC1/2-selective inhibitor RGFP233[22] confirmed that suppression of HDAC1 with HDAC2 was sufficient to induce a significant pro-apoptotic response in Eμ-*Myc* lymphoma.

We have previously demonstrated that FDA-approved compounds, such as vorinostat and panobinostat, that inhibit class I and class II HDACs, and romidepsin that more selectively targets HDACs 1, 2, and 3, all induce apoptosis of Eμ-*Myc* lymphoma and that this biological response is important for the therapeutic effects of these agents in our preclinical models.[29,39,63,64] Collectively, these data suggest that apoptosis mediated by concomitant inhibition of HDACs 1 and 2 is the dominant biological effect mediated by these agents; however,

Figure 6 (continued) demonstrates that RGFP966 treatment increases the population of mature vs immature cells in vitro (×60 magnification; ×4 representative cytospins; (top left) dimethylsulfoxide (DMSO); (top right) 0.05 μM RGFP966; (bottom left) 0.1 μM RGFP966; (bottom right) 0.5 μM RGFP966). At least 300 cells were scanned for each case (n = 3 biological replicates). (E) Calculated percentage of mature and immature cells following treatment with 0.05 μM, 0.1 μM, or 0.5 μM RGFP966. In addition, APL cells treated with RGFP966 at indicated concentrations were immunophenotyped by flow cytometry. (F) An increased percentage of cells positive for Gr.1(Ly-6G) or Mac.1 (CD11b) confirms that low concentrations of RGFP966 triggers differentiation in APL cells similar to *Hdac3* depletion (n = 2 biological replicates).

additional biological responses such as suppression of cell proliferation through HDAC3 inhibition may be important in situations where the apoptotic response is inactivated.

In conclusion, this is the first study to provide comprehensive genetic and pharmacological analyses of the sensitivities of 3 distinct hematological tumor types to suppression of individual *Hdac* isoforms in vitro and in vivo. Using advanced genetic techniques and pharmacological inhibitors, we demonstrated that depletion of *Hdac*3 reduces the proliferation and/or triggers the differentiation of tumor cells in the absence of an apoptotic response. Moreover, although depletion of *Hdac*3 did not synergize with loss of any other *Hdac*s, the combined loss of *Hdac*1 with *Hdac*2 induced potent pro-apoptotic effects demonstrated both in vitro and in vivo. Taken together, our data suggest that HDAC3-selective inhibitors may be effective for the treatment of hematological malignancies and that newly developed agents should prioritize HDAC1 and HDAC2 as targets to induce effective antitumor responses.

Acknowledgments

The authors acknowledge Ross Dickins, Katie McJunkin, Amy Rappaport, Chris Clarke, and Edwin Hawkins for valuable discussion and reagents; Viki Milovac, Sophie Curcio, Ralph Rossi, and Mandy Ludford-Menting for flow cytometry support; and Lauren Dawes and Kat Papastratos for animal husbandry. We acknowledge Oronza A. Botrugno for technical assistance and Giancarlo Pruneri for hematological analysis.

This work was supported by a National Health and Medical Research Council (NHMRC) Biomedical Fellowship and a Peter MacCallum Cancer Foundation Grant (G.M.M.); a Fondazione Italiana per la ricerca sul cancro (FIRC) fellowship (P.M.); National Institutes of Health (grant CA174793), Burroughs-Wellcome Fund Career Award for Medical Scientists, and Alex's Lemonade Stand Foundation "A" Award (C.R.V.); and NHMRC Program and Project Grants (Senior Principal Research Fellow), Cancer Council Victoria, Leukemia Foundation of Australia, Victorian Cancer Agency, and Australian Rotary Health Foundation (R.W.J.). Laboratory research is funded by an ERC Starting Grant (36860), Special Research Program of the Austrian Science Fund (grant F4710), and Boehringer Ingelheim (J.Z.); the Italian Association for Cancer Research, FIRC, National Research Council Flagship Project Epigen, and European Community (4D Cell Fate Project 277899) (S.M.).

Authorship

Contribution: G.M.M. designed experiments, executed research, analyzed and interpreted all data, and wrote the manuscript; L.A.C., K.J.F., and K.S. aided in experimental work in Eμ-*Myc* lymphoma; E.V. and K.S. aided in animal experiments; P.M., F.S., and S.M. designed and executed experiments in acute promyelocytic leukemia cells; J.Z. provided critical experimental reagents; C.R.V. and J.Z. designed and analyzed experiments in acute myeloid leukemia (AML) cells. E.W. and M.R. performed experiments in AML and analyzed data; C.M.H. provided mass spectrometry biomarker analysis; R.W.J., S.M., and J.Z. designed experiments, provided discussion, and assisted in writing the manuscript; and J.R.R. provided RGFP966 and RGFP233 for experimental work.

Conflict-of-interest disclosure: James Rusche is an employee of Repligen Corporation. The other authors declare that there are no other conflicts of interest.

Correspondence: Geoffrey M. Matthews, Department of Medical Oncology, Dana-Farber Cancer Institute, Department of Medicine, Harvard Medical School, 450 Brookline Ave, Harvard Institutes of Medicine Building, Boston, MA 02215; e-mail: geoffreym_matthews@dfci.harvard.edu; Ricky W. Johnstone, Cancer Therapeutics and Cancer Immunology Programs, Peter MacCallum Cancer Centre, St Andrews Place, East Melbourne, VIC 3002, Australia; e-mail: ricky.johnstone@petermac.org; and Saverio Minucci, Drug Development Program and Department of Experimental Oncology, European Institute of Oncology, IEO, 20139 Milan, Italy; e-mail: saverio.minucci@ieo.eu.

References

1. Falkenberg KJ, Johnstone RW. Histone deacetylases and their inhibitors in cancer, neurological diseases and immune disorders. *Nat Rev Drug Discov.* 2014;13(9):673-691.
2. West AC, Johnstone RW. New and emerging HDAC inhibitors for cancer treatment. *J Clin Invest.* 2014;124(1):30-39.
3. Bantscheff M, Hopf C, Savitski MM, et al. Chemoproteomics profiling of HDAC inhibitors reveals selective targeting of HDAC complexes. *Nat Biotechnol.* 2011;29(3):255-265.
4. Dawson MA, Kouzarides T. Cancer epigenetics: from mechanism to therapy. *Cell.* 2012;150(1):12-27.
5. Stengel KR, Hiebert SW, Class I. Class I HDACs affect DNA replication, repair, and chromatin structure: implications for cancer therapy. *Antioxid Redox Signal.* 2015;23(1):51-65.
6. Xu W, Li Y, Liu C, Zhao S. Protein lysine acetylation guards metabolic homeostasis to fight against cancer. *Oncogene.* 2014;33(18):2279-2285.
7. Baylin SB, Ohm JE. Epigenetic gene silencing in cancer - a mechanism for early oncogenic pathway addiction? *Nat Rev Cancer.* 2006;6(2):107-116.
8. Odenike O, Halpern A, Godley LA, et al. A phase I and pharmacodynamic study of the histone deacetylase inhibitor belinostat plus azacitidine in advanced myeloid neoplasia. *Invest New Drugs.* 2015;33(2):371-379.
9. Ghobrial IM, Campigotto F, Murphy TJ, et al. Results of a phase 2 trial of the single-agent histone deacetylase inhibitor panobinostat in patients with relapsed/refractory Waldenström macroglobulinemia. *Blood.* 2013;121(8):1296-1303.
10. Richardson PG, Schlossman RL, Alsina M, et al. PANORAMA 2: panobinostat in combination with bortezomib and dexamethasone in patients with relapsed and bortezomib-refractory myeloma. *Blood.* 2013;122(14):2331-2337.
11. San-Miguel JF, Richardson PG, Günther A, et al. Phase Ib study of panobinostat and bortezomib in relapsed or relapsed and refractory multiple myeloma. *J Clin Oncol.* 2013;31(29):3696-3703.
12. Rasheed W, Bishton M, Johnstone RW, Prince HM. Histone deacetylase inhibitors in lymphoma and solid malignancies. *Expert Rev Anticancer Ther.* 2008;8(3):413-432.
13. Bolden JE, Peart MJ, Johnstone RW. Anticancer activities of histone deacetylase inhibitors. *Nat Rev Drug Discov.* 2006;5(9):769-784.
14. Witt O, Deubzer HE, Milde T, Oehme I. HDAC family: what are the cancer relevant targets? *Cancer Lett.* 2009;277(1):8-21.
15. Buchwald M, Krämer OH, Heinzel T. HDACi—targets beyond chromatin. *Cancer Lett.* 2009;280(2):160-167.
16. Glozak MA, Sengupta N, Zhang X, Seto E. Acetylation and deacetylation of non-histone proteins. *Gene.* 2005;363:15-23.
17. Legartová S, Stixová L, Strnad H, et al. Basic nuclear processes affected by histone acetyltransferases and histone deacetylase inhibitors. *Epigenomics.* 2013;5(4):379-396.
18. Yang Y, Rao R, Shen J, et al. Role of acetylation and extracellular location of heat shock protein 90alpha in tumor cell invasion. *Cancer Res.* 2008;68(12):4833-4842.
19. Johnstone RW, Licht JD. Histone deacetylase inhibitors in cancer therapy: is transcription the primary target? *Cancer Cell.* 2003;4(1):13-18.
20. Ononye SN, van Heyst M, Falcone EM, Anderson AC, Wright DL. Toward isozyme-selective inhibitors of histone deacetylase as therapeutic agents for the treatment of cancer. *Pharm Pat Anal.* 2012;1(2):207-221.

21. Minami J, Suzuki R, Mazitschek R, et al. Histone deacetylase 3 as a novel therapeutic target in multiple myeloma. *Leukemia.* 2014;28(3): 680-689.
22. Wells CE, Bhaskara S, Stengel KR, et al. Inhibition of histone deacetylase 3 causes replication stress in cutaneous T cell lymphoma. *PLoS One.* 2013;8(7):e68915.
23. Balasubramanian S, Verner E, Buggy JJ. Isoform-specific histone deacetylase inhibitors: the next step? *Cancer Lett.* 2009;280(2):211-221.
24. Newbold A, Salmon JM, Martin BP, Stanley K, Johnstone RW. The role of p21(waf1/cip1) and p27(Kip1) in HDACi-mediated tumor cell death and cell cycle arrest in the Eμ-myc model of B-cell lymphoma. *Oncogene.* 2014;33(47):5415-5423.
25. Wilson AJ, Byun DS, Popova N, et al. Histone deacetylase 3 (HDAC3) and other class I HDACs regulate colon cell maturation and p21 expression and are deregulated in human colon cancer. *J Biol Chem.* 2006;281(19):13548-13558.
26. Zuber J, Shi J, Wang E, et al. RNAi screen identifies Brd4 as a therapeutic target in acute myeloid leukaemia. *Nature.* 2011;478(7370): 524-528.
27. Minucci S, Monestiroli S, Giavara S, et al. PML-RAR induces promyelocytic leukemias with high efficiency following retroviral gene transfer into purified murine hematopoietic progenitors. *Blood.* 2002;100(8):2989-2995.
28. Santoro F, Botrugno OA, Dal Zuffo R, et al. A dual role for Hdac1: oncosuppressor in tumorigenesis, oncogene in tumor maintenance. *Blood.* 2013; 121(17):3459-3468.
29. Newbold A, Matthews GM, Bots M, et al. Molecular and biologic analysis of histone deacetylase inhibitors with diverse specificities. *Mol Cancer Ther.* 2013;12(12):2709-2721.
30. Vert J-P, Foveau N, Lajaunie C, Vandenbrouck Y. An accurate and interpretable model for siRNA efficacy prediction. *BMC Bioinformatics.* 2006; 7(1):520.
31. Matthews GM, Lefebure M, Doyle MA, et al. Preclinical screening of histone deacetylase inhibitors combined with ABT-737, rhTRAIL/MD5-1 or 5-azacytidine using syngeneic Vk*MYC multiple myeloma. *Cell Death Dis.* 2013;4:e798.
32. Turgeon ML. Clinical Hematology: Theory and Procedures. Hagerstown, MD: Lippincott Williams & Wilkins; 2005:67.
33. Zuber J, Rappaport AR, Luo W, et al. An integrated approach to dissecting oncogene addiction implicates a Myb-coordinated self-renewal program as essential for leukemia maintenance [published correction appears in *Genes Dev.* 2011;25(18):1997]. *Genes Dev.* 2011;25(15):1628-1640.
34. Zuber J, McJunkin K, Fellmann C, et al. Toolkit for evaluating genes required for proliferation and survival using tetracycline-regulated RNAi. *Nat Biotechnol.* 2011;29(1):79-83.
35. Malvaez M, McQuown SC, Rogge GA, et al. HDAC3-selective inhibitor enhances extinction of cocaine-seeking behavior in a persistent manner. *Proc Natl Acad Sci USA.* 2013;110(7):2647-2652.
36. Summers AR, Fischer MA, Stengel KR, et al. HDAC3 is essential for DNA replication in hematopoietic progenitor cells. *J Clin Invest.* 2013;123(7):3112-3123.
37. Dow LE, Premsrirut PK, Zuber J, et al. A pipeline for the generation of shRNA transgenic mice. *Nat Protoc.* 2012;7(2):374-393.
38. Dow LE, Nasr Z, Saborowski M, et al. Conditional reverse tet-transactivator mouse strains for the efficient induction of TRE-regulated transgenes in mice. *PLoS One.* 2014;9(4):e95236.
39. Lindemann RK, Newbold A, Whitecross KF, et al. Analysis of the apoptotic and therapeutic activities of histone deacetylase inhibitors by using a mouse model of B cell lymphoma. *Proc Natl Acad Sci USA.* 2007;104(19):8071-8076.
40. Huang W, Tan D, Wang X, et al. Histone deacetylase 3 represses p15(INK4b) and p21 (WAF1/cip1) transcription by interacting with Sp1. *Biochem Biophys Res Commun.* 2006;339(1): 165-171.
41. Jiao F, Hu H, Yuan C, et al. Histone deacetylase 3 promotes pancreatic cancer cell proliferation, invasion and increases drug-resistance through histone modification of P27, P53 and Bax. *Int J Oncol.* 2014;45(4):1523-1530.
42. Feng L, Pan M, Sun J, et al. Histone deacetylase 3 inhibits expression of PUMA in gastric cancer cells. *J Mol Med (Berl).* 2013;91(1):49-58.
43. Singh N, Gupta M, Trivedi CM, Singh MK, Li L, Epstein JA. Murine craniofacial development requires Hdac3-mediated repression of Msx gene expression. *Dev Biol.* 2013;377(2):333-344.
44. Fajas L, Egler V, Reiter R, et al. The retinoblastoma-histone deacetylase 3 complex inhibits PPARgamma and adipocyte differentiation. *Dev Cell.* 2002;3(6):903-910.
45. Fajas L, Egler V, Reiter R, Miard S, Lefebvre AM, Auwerx J. PPARgamma controls cell proliferation and apoptosis in an RB-dependent manner. *Oncogene.* 2003;22(27):4186-4193.
46. Dickins RA, Hemann MT, Zilfou JT, et al. Probing tumor phenotypes using stable and regulated synthetic microRNA precursors. *Nat Genet.* 2005; 37(11):1289-1295.
47. Barna M, Pusic A, Zollo O, et al. Suppression of Myc oncogenic activity by ribosomal protein haploinsufficiency. *Nature.* 2008;456(7224): 971-975.
48. Teng T, Mercer CA, Hexley P, Thomas G, Fumagalli S. Loss of tumor suppressor RPL5/ RPL11 does not induce cell cycle arrest but impedes proliferation due to reduced ribosome content and translation capacity. *Mol Cell Biol.* 2013;33(23):4660-4671.
49. Spurling CC, Godman CA, Noonan EJ, Rasmussen TP, Rosenberg DW, Giardina C. HDAC3 overexpression and colon cancer cell proliferation and differentiation. *Mol Carcinog.* 2008;47(2):137-147.
50. Chen S, Zhao Y, Gou WF, Zhao S, Takano Y, Zheng HC. The anti-tumor effects and molecular mechanisms of suberoylanilide hydroxamic acid (SAHA) on the aggressive phenotypes of ovarian carcinoma cells. *PLoS One.* 2013;8(11):e79781.
51. Gravina GL, Marampon F, Giusti I, et al. Differential effects of PXD101 (belinostat) on androgen-dependent and androgen-independent prostate cancer models. *Int J Oncol.* 2012;40(3): 711-720.
52. Hsieh YJ, Hwu L, Chen YC, et al. P21-driven multifusion gene system for evaluating the efficacy of histone deacetylase inhibitors by in vivo molecular imaging and for transcription targeting therapy of cancer mediated by histone deacetylase inhibitor. *J Nucl Med.* 2014;55(4): 678-685.
53. Grimwade D, Mistry AR, Solomon E, Guidez F. Acute promyelocytic leukemia: a paradigm for differentiation therapy. *Cancer Treat Res.* 2010; 145:219-235.
54. Minucci S, Nervi C, Lo Coco F, Pelicci PG. Histone deacetylases: a common molecular target for differentiation treatment of acute myeloid leukemias? *Oncogene.* 2001;20(24):3110-3115.
55. Dasmahapatra G, Patel H, Friedberg J, Quayle SN, Jones SS, Grant S. In vitro and in vivo interactions between the HDAC6 inhibitor ricolinostat (ACY1215) and the irreversible proteasome inhibitor carfilzomib in non-Hodgkin lymphoma cells. *Mol Cancer Ther.* 2014;13(12): 2886-2897.
56. Hideshima T, Bradner JE, Wong J, et al. Small-molecule inhibition of proteasome and aggresome function induces synergistic antitumor activity in multiple myeloma. *Proc Natl Acad Sci USA.* 2005; 102(24):8567-8572.
57. Santo L, Hideshima T, Kung AL, et al. Preclinical activity, pharmacodynamic, and pharmacokinetic properties of a selective HDAC6 inhibitor, ACY-1215, in combination with bortezomib in multiple myeloma. *Blood.* 2012;119(11):2579-2589.
58. Ding N, Ping L, Feng L, Zheng X, Song Y, Zhu J. Histone deacetylase 6 activity is critical for the metastasis of Burkitt's lymphoma cells. *Cancer Cell Int.* 2014;14(1):139.
59. Haggarty SJ, Koeller KM, Wong JC, Grozinger CM, Schreiber SL. Domain-selective small-molecule inhibitor of histone deacetylase 6 (HDAC6)-mediated tubulin deacetylation. *Proc Natl Acad Sci USA.* 2003;100(8):4389-4394.
60. Zhang L, Liu N, Xie S, et al. HDAC6 regulates neuroblastoma cell migration and may play a role in the invasion process. *Cancer Biol Ther.* 2014; 15(11):1561-1570.
61. Senese S, Zaragoza K, Minardi S, et al. Role for histone deacetylase 1 in human tumor cell proliferation. *Mol Cell Biol.* 2007;27(13): 4784-4795.
62. Wilting RH, Yanover E, Heideman MR, et al. Overlapping functions of Hdac1 and Hdac2 in cell cycle regulation and haematopoiesis. *EMBO J.* 2010;29(15):2586-2597.
63. Ellis L, Bots M, Lindemann RK, et al. The histone deacetylase inhibitors LAQ824 and LBH589 do not require death receptor signaling or a functional apoptosome to mediate tumor cell death or therapeutic efficacy. *Blood.* 2009;114(2):380-393.
64. Peart MJ, Tainton KM, Ruefli AA, et al. Novel mechanisms of apoptosis induced by histone deacetylase inhibitors. *Cancer Res.* 2003;63(15): 4460-4471.